Non-Degenerate Two-Photon Absorption Cross Section for the $6S_{1/2} \rightarrow 8S_{1/2}$ Transition in Cesium Atoms

Catalina Fuentes Rubio* and Mayerlin Núñez Portela†

Grupo de Óptica Cuántica, Departamento de Física,

Universidad de los Andes, Bogotá, Colombia

(Dated: May 23, 2026)

This work presents a theoretical study of non-degenerate two-photon absorption (ND-TPA) in the cesium $6S_{1/2} \rightarrow 8S_{1/2}$ transition. Starting from second-order time-dependent perturbation theory in the electric dipole approximation, an expression for the non-degenerate TPA cross section $\sigma_{\mathrm{ND}}(\omega_1, \omega_2)$ is derived.

The expression is evaluated numerically using the dominant intermediate states $6P_{1/2}$, $6P_{3/2}$, $7P_{1/2}$, and $7P_{3/2}$. The non-degeneracy parameter Ω is introduced through $\omega_1 = \omega_0 - \Omega$ and $\omega_2 = \omega_0 + \Omega$, keeping the total two-photon energy fixed. The results show that the cross section is strongly enhanced when one photon approaches an intermediate resonance and that local minima arise from destructive interference between intermediate-state pathways. In particular, a configuration near the $6P_{3/2}$ resonance predicts an enhancement of approximately 3.4 orders of magnitude relative to the degenerate reference point. These results provide a theoretical basis for identifying frequency configurations that maximize the two-photon cross-section in cesium atoms.

* c.fuentesr@uniandes.edu.co

† m.nunez@uniandes.edu.co

I. INTRODUCTION

Two-photon absorption (*Two-Photon Absorption*, TPA) is a nonlinear optical process in which an atom or molecule transitions from an initial state $|\psi_i\rangle$ to a final state $|\psi_f\rangle$ through the absorption of two photons, and then decays radiatively by emitting fluorescence. This process was theoretically predicted by Maria Göppert-Mayer in 1931 [1] and experimentally observed thirty years later, after the development of the laser [2].

The fundamental condition for the transition to occur is energy conservation. The sum of the energies of the two absorbed photons must match the energy difference between the initial and final states:

$$E_f - E_i \;=\; \hbar\omega_1 + \hbar\omega_2, \tag{1}$$

where E_i and E_f are the energies of the initial and final atomic states, and $\hbar\omega_1 = E_1$, $\hbar\omega_2 = E_2$ are the energies of the incident photons. Equivalently, $\omega_{fi} \equiv (E_f - E_i)/\hbar \simeq \omega_1 + \omega_2$.

From this condition, two regimes can be distinguished. In the degenerate case, both photons have the same frequency, $\omega_1 = \omega_2 \equiv \omega$, so that the resonance condition is written as $2\omega \simeq \omega_{fi}$. In the non-degenerate case, the photons have different frequencies, $\omega_1 \neq \omega_2$, but their sum still satisfies the same resonance condition. This difference is illustrated in Figure 1. After excitation to the final state, the atom decays radiatively and emits fluorescence photons, which constitute the signal measured in the laboratory.

The quantity that quantifies the probability that the process occurs is the two-photon absorption cross section, σ. This quantity depends on the electronic structure of the system and on the frequencies of the absorbed photons [3]. For this reason, comparing the cross section in the degenerate and non-degenerate regimes makes it possible to study how the optical response of the atom changes when the same total energy is distributed differently between the two photons.

The TPA cross section has been studied experimentally in atomic vapors. For the degenerate case, Caracas Núñez *et al.* measured and calculated the cross section of the $6S_{1/2} \rightarrow 8S_{1/2}$ transition in cesium atoms, using TPA-induced fluorescence in a vapor cell [5]. In the non-degenerate regime, Bjorkholm and Liao demonstrated in sodium vapor that the two-photon absorption cross

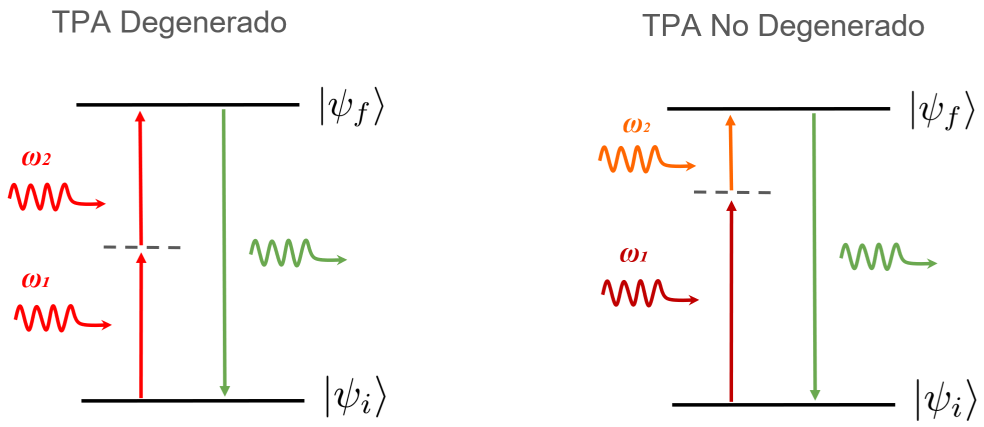

FIG. 1. Comparison between degenerate TPA (left) and non-degenerate TPA (right). In the degenerate case, both photons have the same frequency. In the non-degenerate case, the frequencies are different, but the sum $\omega_1 + \omega_2$ remains equal to ω_{fi}. This additional freedom makes it possible to bring one of the frequencies close to a real intermediate resonance of the atom while keeping the two-photon resonance fixed.

section can increase by more than seven orders of magnitude when one of the frequencies is tuned near a real intermediate state [8]. In a later work, the same authors developed a detailed theoretical treatment of the line shape and strength of two-photon absorption in the presence of a resonant or nearly resonant intermediate state [9]. More recently, True *et al.* studied two-color two-photon absorption in rubidium, scanning the detuning with respect to the intermediate state and comparing the measured rates with the theoretically expected behavior [10]. These results show that the non-degenerate regime makes it possible to control the transition amplitude through the proximity to intermediate resonances.

The cesium atom (^{133}Cs) is a convenient system for this type of study. Since it is an alkali atom with a single valence electron, its structure allows for a relatively controlled theoretical treatment and, at the same time, its optical transitions are experimentally accessible with commercial diode lasers. In particular, the $6S_{1/2} \rightarrow 8S_{1/2}$ two-photon transition has a wavelength close to 822 nm [7], which makes it possible to study it with the elements available in the Quantum Optics laboratory. The cesium energy level diagram is shown in Figure 2.

For this transition, the degenerate case constitutes the natural reference point. Starting from

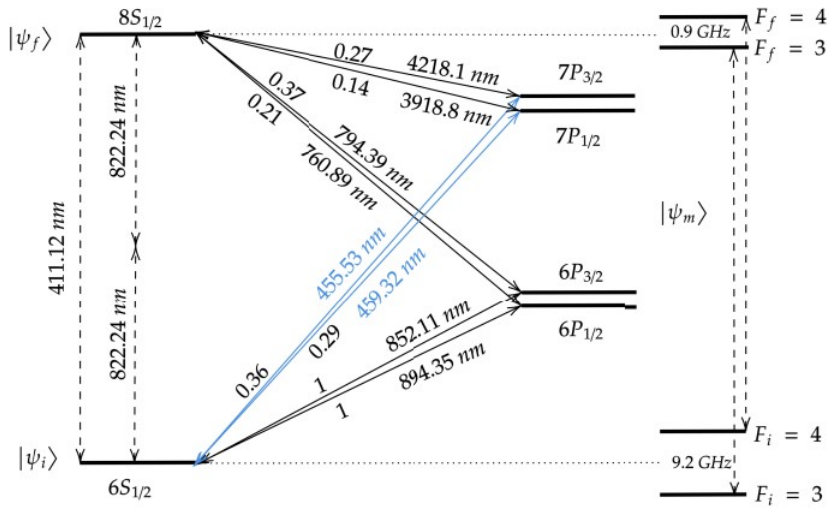

FIG. 2. Cesium energy levels relevant to this work. Solid lines represent one-photon transitions. Dashed lines indicate two-photon transitions. Taken from [5].

second-order time-dependent perturbation theory and averaging over the orientations of the atom with respect to the field polarization, Caracas Núñez *et al.* obtained the following expression for the degenerate cross section [5]:

$$\sigma_D(\omega) \;=\; \frac{\mu_0\, e^4\, \omega}{2\varepsilon_0\, \hbar^3}\; \frac{\gamma_f}{(\omega_{fi}-2\omega)^2+\gamma_f^2/4}\; \left|\sum_m \frac{\mu_{fm}\,\mu_{mi}}{\omega_{mi}-\omega}\right|^2, \tag{2}$$

where $\omega = 2\pi\nu$ is the angular frequency of the laser, ω_{fi} is the transition frequency, γ_f is the natural linewidth of the $8S_{1/2}$ level, and $\mu_{ab} = \langle a|\,\hat{\boldsymbol{\epsilon}}\cdot\hat{\mathbf{r}}\,|b\rangle$ are the dipole matrix elements projected onto the field polarization. The sum over m runs over the dominant intermediate states $\{6P_{1/2}, 6P_{3/2}, 7P_{1/2}, 7P_{3/2}\}$, indicated in Figure 2.

By evaluating this expression for the atomic parameters of cesium in the Doppler-free limit, Ref. [5] reports the theoretical value

$$\sigma_D \;=\; 4.58\times10^{-21}\ \mathrm{cm}^4/\mathrm{W}, \tag{3}$$

which constitutes the natural reference point for the present calculation.

In the non-degenerate regime, the total energy delivered to the atom remains the same, but it is distributed asymmetrically between the two photons. To describe this distribution, the non-degeneracy parameter Ω is introduced:

$$\omega_1 = \omega_0 - \Omega, \qquad \omega_2 = \omega_0 + \Omega, \qquad \omega_0 \equiv \frac{\omega_{fi}}{2}. \tag{4}$$

When $\Omega = 0$, the degenerate case is recovered. As Ω increases, the frequencies separate symmetrically around ω_0, but their sum remains fixed: $\omega_1 + \omega_2 = \omega_{fi}$, as shown in Figure 3.

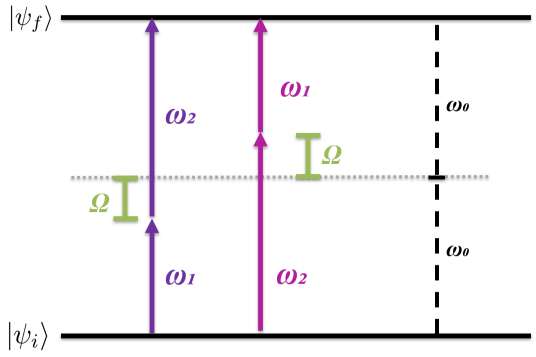

FIG. 3. Illustration of non-degenerate TPA in terms of the non-degeneracy parameter Ω. The two photons are separated symmetrically around the central frequency $\omega_0 = \omega_{fi}/2$, so that their sum remains fixed at ω_{fi}. When $\Omega = 0$, the degenerate case is recovered.

Varying Ω makes it possible to explore how the TPA response changes when one of the frequencies approaches a real intermediate transition of the atom, such as the $6S_{1/2} \rightarrow 6P_{3/2}$ transition in Figure 2. In this situation, the TPA cross section can increase significantly. This effect is known as *intermediate-state resonance enhancement* and has been experimentally observed in sodium vapor [8] and in rubidium vapor [10], where the TPA signal can change by several orders of magnitude when the frequency of one of the photons is brought close to an intermediate transition.

Taking the above into account, this project proposes to study the two-photon absorption cross section in the non-degenerate regime for the $6S_{1/2} \rightarrow 8S_{1/2}$ transition in cesium. In particular, the goal is to derive a theoretical expression for the non-degenerate cross section and evaluate how it changes when one of the photon frequencies is tuned close to an intermediate state. This analysis will make it possible to determine whether the non-degenerate regime can enhance the TPA cross section relative to the degenerate case, providing a theoretical basis for future studies involving weak optical signals, such as entangled two-photon absorption (ETPA), where the expected counts are much smaller due to the low flux of entangled photon pairs [12].

II. DERIVATION OF THE NON-DEGENERATE TPA CROSS SECTION

The starting point is the standard treatment of an atom interacting with a classical electromagnetic field within the electric dipole approximation. The whole derivation proceeds in five steps: (i) second-order time-dependent perturbation theory to obtain a generic transition amplitude, (ii) specialization of the field to two distinct frequencies, (iii) identification of the two time-ordered absorption paths and construction of the non-degenerate transition amplitude, (iv) calculation of the probability and transition rate including the interference between paths, and (v) conversion of the rate into a cross section.

A. Second-Order Time-Dependent Perturbation Theory

We work in the interaction picture and treat the atom-field interaction as a small perturbation. The quantity we want to calculate is the transition amplitude from the initial atomic state $|i\rangle$ to the final atomic state $|f\rangle$. In the interaction picture, this amplitude is given by the projection of the evolved initial state onto the final state:

$$A_{i\to f}(t) = \langle f|\, \hat{U}^{(I)}(t,t_0)\, |i\rangle\,. \tag{5}$$

Therefore, calculating the transition amplitude reduces to finding the time-evolution operator $\hat{U}^{(I)}(t,t_0)$ associated with the atom-field interaction.

In the electric dipole approximation, the interaction Hamiltonian is

$$\hat{H}_{\rm int}(t) = -e\,\hat{\mathbf{r}}\cdot\mathbf{E}(t), \tag{6}$$

where e is the elementary charge, $\hat{\mathbf{r}}$ is the position operator, and $\mathbf{E}(t)$ is the classical electric field. This approximation is well justified for the optical wavelengths involved ($\lambda \sim$ 800–900 nm), for which the spatial variation of the field over the atom is negligible ($\mathbf{k}\cdot\hat{\mathbf{r}} \ll 1$).

The time evolution of the atomic state is governed by the Dyson series for the time-evolution operator. Expanding to second order,

$$\hat{U}^{(I)}(t,t_0) = \mathbb{I} - \frac{i}{\hbar}\int_{t_0}^{t} dt'\,\hat{H}_{\rm int}(t') + \left(-\frac{i}{\hbar}\right)^2 \int_{t_0}^{t} dt' \int_{t_0}^{t'} dt''\,\hat{H}_{\rm int}(t')\,\hat{H}_{\rm int}(t'') + \cdots\,. \tag{7}$$

Substituting this expansion into Eq. (5) gives the transition amplitude as a perturbative series. The zeroth-order term only gives the overlap between the initial and final states, while the first-order term describes one interaction with the field and therefore mediates one-photon transitions.

Since TPA requires two interactions with the field, the lowest non-vanishing contribution to the two-photon transition amplitude comes from the second-order term:

$$A^{(2)}_{i\to f}(t) = \langle f|\, \hat{U}^{(I,2)}(t,t_0)\, |i\rangle\,, \tag{8}$$

with

$$\hat{U}^{(I,2)}(t,t_0) = \left(-\frac{i}{\hbar}\right)^2 \int_{t_0}^{t} dt' \int_{t_0}^{t'} dt''\, \hat{H}_{\rm int}(t')\, \hat{H}_{\rm int}(t''). \tag{9}$$

Thus,

$$A^{(2)}_{i\to f}(t) = \left(-\frac{i}{\hbar}\right)^2 \int_{t_0}^{t} dt' \int_{t_0}^{t'} dt''\ \langle f|\, \hat{H}_{\rm int}(t')\, \hat{H}_{\rm int}(t'')\, |i\rangle\,. \tag{10}$$

This expression shows explicitly why the time-evolution operator is needed: the two-photon amplitude is obtained from the second-order term in the expansion of $\hat{U}^{(I)}$.

To make the role of the intermediate states explicit, we insert the closure relation over a complete set of atomic states,

$$\mathbb{I} = \sum_m |m\rangle\, \langle m|\,. \tag{11}$$

Taking $t_0 = 0$, the second-order transition amplitude becomes

$$A^{(2)}_{i\to f}(t) = \left(-\frac{i}{\hbar}\right)^2 \sum_m \int_0^{t} dt' \int_0^{t'} dt''\ \langle f|\, \hat{H}_{\rm int}(t')\, |m\rangle\ \langle m|\, \hat{H}_{\rm int}(t'')\, |i\rangle\ e^{i\omega_{fm}t'} e^{i\omega_{mi}t''}, \tag{12}$$

where $\omega_{ab} = (E_a - E_b)/\hbar$. The sum extends over the intermediate states $|m\rangle$ through which the system can virtually pass between the absorption of the first and the second photon. In practice, only the intermediate states whose energies lie close to one of the photon energies contribute appreciably to the sum. For the cesium $6S_{1/2} \to 8S_{1/2}$ transition, the dominant intermediate states are the four nearest nP levels $6P_{1/2}$, $6P_{3/2}$, $7P_{1/2}$, $7P_{3/2}$, which are shown in Figure 2.

B. Non-Degenerate Electric Field

For the non-degenerate regime the laser field contains two frequency components,

$$\mathbf{E}(t) = \frac{E_1}{2}\left(e^{-i\omega_1 t} + e^{i\omega_1 t}\right)\hat{\boldsymbol{\epsilon}}_1 + \frac{E_2}{2}\left(e^{-i\omega_2 t} + e^{i\omega_2 t}\right)\hat{\boldsymbol{\epsilon}}_2, \tag{13}$$

where E_1 and E_2 are the real amplitudes of the two beams and $\hat{\boldsymbol{\epsilon}}_1$, $\hat{\boldsymbol{\epsilon}}_2$ their polarization unit vectors. Substituting Eq. (13) into Eq. (6) produces four terms per photon: two associated with absorption

($e^{-i\omega_j t}$) and two with emission ($e^{+i\omega_j t}$). For a two-photon absorption process only the absorption terms are kept, since the emission terms oscillate at $\omega_{ab} + \omega_j$ and do not satisfy the resonance condition (1). Under this rotating-wave-type simplification the relevant part of the interaction Hamiltonian becomes

$$\hat{H}_{\rm int}(t) = -\frac{eE_1}{2}\,\hat{\boldsymbol{\epsilon}}_1 \cdot \hat{\mathbf{r}}\, e^{-i\omega_1 t} - \frac{eE_2}{2}\,\hat{\boldsymbol{\epsilon}}_2 \cdot \hat{\mathbf{r}}\, e^{-i\omega_2 t}. \tag{14}$$

C. Transition Amplitude with Two Time Orderings

Substituting Eq. (14) into the second-order amplitude (12) yields four contributions, corresponding to the four possible combinations of absorbing photons of frequency ω_1 or ω_2 at times t'' and t'. Two of these, A_{11} and A_{22}, describe the absorption of two photons of the same frequency and resonate at $2\omega_1 \simeq \omega_{fi}$ and $2\omega_2 \simeq \omega_{fi}$ respectively; for $\omega_1 \neq \omega_2$ they are far from resonance and contribute negligibly. The non-degenerate amplitude therefore reduces to the two cross terms,

$$A^{\rm ND}_{i\to f}(t) = A_{12}(t) + A_{21}(t), \tag{15}$$

each of which represents one of the two indistinguishable time orderings of the absorption process:

$$A_{12}: \quad |i\rangle \xrightarrow{\omega_2} |m\rangle \xrightarrow{\omega_1} |f\rangle\,, \tag{16}$$

$$A_{21}: \quad |i\rangle \xrightarrow{\omega_1} |m\rangle \xrightarrow{\omega_2} |f\rangle\,. \tag{17}$$

Defining the projected dipole matrix elements $\mu^{(j)}_{ab} \equiv \langle a|\,\hat{\boldsymbol{\epsilon}}_j \cdot \hat{\mathbf{r}}\,|b\rangle$, the explicit time-dependent expressions are

$$A_{12}(t) = \frac{e^2 E_1 E_2}{4\hbar^2} \sum_m \frac{\mu^{(1)}_{fm}\,\mu^{(2)}_{mi}}{\omega_{mi} - \omega_2} \left[\frac{e^{i(\omega_{fi} - \omega_1 - \omega_2)t} - 1}{\omega_{fi} - \omega_1 - \omega_2} - \frac{e^{i(\omega_{fm} - \omega_1)t} - 1}{\omega_{fm} - \omega_1} \right], \tag{18}$$

$$A_{21}(t) = \frac{e^2 E_1 E_2}{4\hbar^2} \sum_m \frac{\mu^{(2)}_{fm}\,\mu^{(1)}_{mi}}{\omega_{mi} - \omega_1} \left[\frac{e^{i(\omega_{fi} - \omega_1 - \omega_2)t} - 1}{\omega_{fi} - \omega_1 - \omega_2} - \frac{e^{i(\omega_{fm} - \omega_2)t} - 1}{\omega_{fm} - \omega_2} \right]. \tag{19}$$

Each amplitude contains two oscillatory contributions. The first term in each bracket peaks at the two-photon resonance $\omega_1 + \omega_2 \simeq \omega_{fi}$ and is responsible for the global TPA signal. The second term peaks when one of the photons brings the intermediate level into resonance, $\omega_j \simeq \omega_{fm}$. Both amplitudes share the same final state $|f\rangle$, so A_{12} and A_{21} correspond to indistinguishable quantum paths and must be added coherently [4].

D. Probability and Transition Rate

Because the two paths reach the same final state, the total transition probability is obtained from the square modulus of the coherent sum:

$$p_{\mathrm{ND}}(t) = |A_{12}(t) + A_{21}(t)|^2 = |A_{12}|^2 + |A_{21}|^2 + 2\,\mathrm{Re}[A_{12}A_{21}^*]\,. \tag{20}$$

The first two terms are the individual probabilities of each ordering; the third is a quantum interference term. As will be shown in Section III, this interference is responsible for the destructive minima (Fano-like valleys) that appear between consecutive intermediate-state resonances.

The transition rate is the time derivative of the probability,

$$\Gamma_{\mathrm{ND}} = \frac{dp_{\mathrm{ND}}}{dt}. \tag{21}$$

In the long-time limit the temporal factors in Eqs. (18)–(19) converge to sharply peaked functions, which in the presence of finite-lifetime broadening become Lorentzian line shapes [3, 4]:

$$\lim_{t\to\infty} \frac{\sin^2[(\omega-\omega_0)t/2]}{(\omega-\omega_0)^2/4} \;\longrightarrow\; \frac{\gamma}{(\omega-\omega_0)^2+\gamma^2/4}. \tag{22}$$

Three different linewidths enter: the natural linewidth γ_f of the final state $|8S_{1/2}\rangle$ sets the width of the global two-photon resonance; the natural linewidths γ_m of the intermediate states set the widths of the single-photon resonances; and the cross term $2\,\mathrm{Re}[A_{12}A_{21}^*]$ involves the averaged width $\gamma_{mm'} = (\gamma_m + \gamma_{m'})/2$ when the two paths go through different intermediate states.

E. Non-Degenerate Cross Section

The non-degenerate TPA cross section is defined through the relation between the transition rate and the product of the two beam intensities $I_j = \varepsilon_0 c E_j^2/2$,

$$\Gamma_{\mathrm{ND}} = \frac{\sigma_{\mathrm{ND}}(\omega_1,\omega_2)\, I_1 I_2}{2\hbar^2\omega_1\omega_2}, \tag{23}$$

Combining the results of the previous subsections, the non-degenerate cross section takes the explicit form

$$\begin{aligned}\sigma_{\mathrm{ND}}(\omega_1,\omega_2) = \frac{\mu_0 e^4 \omega_1 \omega_2}{2\varepsilon_0 \hbar^3} \Bigg\{ & \frac{\gamma_f}{(\omega_{fi}-\omega_1-\omega_2)^2+\gamma_f^2/4} \left| \sum_m \left[\frac{\mu^{(1)}_{fm}\mu^{(2)}_{mi}}{\omega_{mi}-\omega_2} + \frac{\mu^{(2)}_{fm}\mu^{(1)}_{mi}}{\omega_{mi}-\omega_1} \right] \right|^2 \\ & + \sum_m \frac{\gamma_m}{(\omega_{fm}-\omega_1)^2+\gamma_m^2/4} \left| \sum_{m'} \frac{\mu^{(1)}_{fm'}\mu^{(2)}_{m'i}}{\omega_{m'i}-\omega_2} \right|^2 \\ & + \sum_m \frac{\gamma_m}{(\omega_{fm}-\omega_2)^2+\gamma_m^2/4} \left| \sum_{m'} \frac{\mu^{(2)}_{fm'}\mu^{(1)}_{m'i}}{\omega_{m'i}-\omega_1} \right|^2 \\ & + 2\,\mathrm{Re} \sum_{m,m'} \frac{\mu^{(1)}_{fm}\mu^{(2)*}_{mi}\,\mu^{(2)}_{fm'}\mu^{(1)}_{m'i}}{(\omega_{mi}-\omega_2)(\omega_{m'i}-\omega_1)} \frac{\gamma_{mm'}}{(\omega_{fm'}-\omega_1-\omega_{fm}+\omega_2)^2+\gamma_{mm'}^2/4} \Bigg\}. \end{aligned} \tag{24}$$

Equation (24) gives the non-degenerate TPA cross section as a sum of resonant contributions associated with the final and intermediate atomic levels. The first term contains the two-photon resonance denominator, centered at $\omega_1 + \omega_2 = \omega_{fi}$, and includes the coherent sum over the two possible absorption orderings. The second and third terms contain one-photon resonance denominators involving the intermediate states, and therefore become important when either ω_1 or ω_2 approaches an allowed nP transition. These terms describe the resonant enhancement of the two-photon response near intermediate levels [9, 10]. The last term is a cross contribution between different intermediate-state pathways and accounts for the interference structure of the spectrum.

For the cesium transition considered here, the sums over m and m' are evaluated over the dominant intermediate states $\{6P_{1/2}, 6P_{3/2}, 7P_{1/2}, 7P_{3/2}\}$. The dependence on the frequency pair (ω_1, ω_2) is analyzed numerically in the next section.

III. NUMERICAL ANALYSIS

In this section the analytic expression (24) is evaluated numerically for cesium atoms. The goal is twofold: to characterize the spectral structure of σ_{ND} as a function of the non-degeneracy parameter Ω, and to quantify the enhancement of the cross section that can be obtained by tuning Ω close to an intermediate resonance.

A. Atomic Parameters and Parametrization

The non-degenerate cross section is evaluated for the cesium $6S_{1/2} \to 8S_{1/2}$ transition, using the four dominant intermediate states $|m\rangle \in \{6P_{1/2}, 6P_{3/2}, 7P_{1/2}, 7P_{3/2}\}$. Transition frequencies, electric dipole matrix elements and natural linewidths are taken from the experimental and theoretical work of Caracas Núñez *et al.* [5, 6], which provides the same atomic input used in the degenerate calculation. The two beams are assumed to be linearly polarized with parallel polarizations, so that $\hat{\boldsymbol{\epsilon}}_1 = \hat{\boldsymbol{\epsilon}}_2$ and the projected dipole matrix elements satisfy $\mu_{ab}^{(1)} = \mu_{ab}^{(2)} \equiv \mu_{ab}$.

To probe the dependence of σ_{ND} on the distribution of energy between the two photons while keeping the two-photon resonance fixed, the symmetric parametrization of Eq. (4) is used:

$$\omega_1 = \omega_0 - \Omega, \qquad \omega_2 = \omega_0 + \Omega, \qquad \omega_0 = \frac{\omega_{fi}}{2}. \tag{25}$$

With this choice $\omega_1 + \omega_2 = \omega_{fi}$ for every Ω, so the global two-photon resonance term in Eq. (24) is always approached. The whole structure of $\sigma_{\mathrm{ND}}(\Omega)$ is then driven by the intermediate-state denominators. The expected positions of the intermediate-state resonances, obtained from the condition $\omega_j(\Omega) = \omega_{mi}$, are

$$\Omega_m = \pm\,(\omega_{mi} - \omega_0), \tag{26}$$

so that each intermediate level $|m\rangle$ produces a pair of symmetric peaks in the spectrum.

B. Spectral Structure of $\sigma_{\mathbf{ND}}(\Omega)$

Figure 4 shows the numerically computed cross section $\sigma_{\mathrm{ND}}(\Omega)$ in the symmetric range $|\Omega|/2\pi \leq 50$ THz, on a logarithmic scale. The curve exhibits the two characteristic features predicted by the analytic expression (24): sharp resonance peaks at the positions given by Eq. (26), and pronounced local minima between consecutive peaks.

The peak centers obtained numerically are in agreement with the analytical prediction of Eq. (26):

$$\Omega/2\pi \simeq \pm 12.8 \text{ THz} \quad (6P_{3/2}), \tag{27}$$

$$\Omega/2\pi \simeq \pm 29.4 \text{ THz} \quad (6P_{1/2}), \tag{28}$$

$$\Omega/2\pi \simeq \pm 288.0 \text{ THz} \quad (7P_{1/2}), \tag{29}$$

$$\Omega/2\pi \simeq \pm 293.4 \text{ THz} \quad (7P_{3/2}). \tag{30}$$

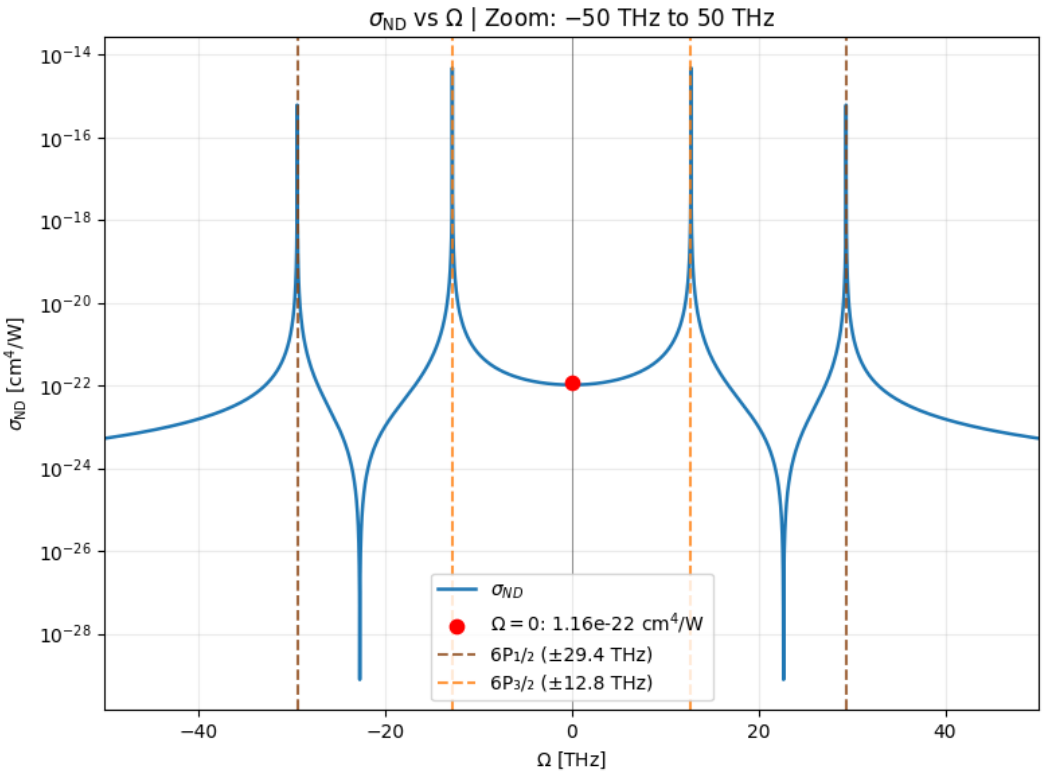

FIG. 4. Non-degenerate TPA cross section $\sigma_{\mathrm{ND}}(\Omega)$ for the cesium $6S_{1/2} \to 8S_{1/2}$ transition, plotted on a logarithmic scale over $|\Omega|/2\pi \leq 50$ THz. Sharp peaks appear when one of the photons approaches the $6P_{3/2}$ ($\Omega/2\pi \simeq \pm 12.8$ THz, dashed orange) or $6P_{1/2}$ ($\Omega/2\pi \simeq \pm 29.4$ THz, dashed brown) intermediate resonances. The red marker indicates the value $\sigma_{\mathrm{ND}}(0) = 1.16 \times 10^{-22}\,\mathrm{cm}^4/\mathrm{W}$, obtained at the degenerate point.

The two outer pairs of resonances (associated with $7P_{1/2}$ and $7P_{3/2}$) lie well outside the range shown in Figure 4 and are dominated in the spectrum by the two inner $6P$ resonances. In a neighbourhood of each peak the line shape is well approximated by a single Lorentzian whose width is set by the natural linewidth γ_m of the corresponding intermediate state; far from the peak, the tails follow the expected $1/\delta^2$ behaviour of the perturbative denominators, where $\delta = \omega_{fm} - \omega_j$ is the detuning from the intermediate level.

Between the $6P_{3/2}$ and $6P_{1/2}$ peaks, $\sigma_{\mathrm{ND}}(\Omega)$ develops a deep local minimum. This minimum is a consequence of the coherent sum inside the global two-photon resonance term of Eq. (24): when a photon frequency ω_j lies between two intermediate transitions, the denominators $\omega_{m_1 i} - \omega_j$ and $\omega_{m_2 i} - \omega_j$ have opposite signs, so the corresponding contributions partially cancel each other. Since σ_{ND} depends on the squared modulus of this sum, the cancellation produces a Fano-like valley [11]. The minima do not reach zero because the dipole matrix elements and the natural linewidths of

the different intermediate states are not equal, so the cancellation is incomplete.

C. Comparison with the Degenerate Reference Value

A natural consistency check of the derivation is the behaviour of $\sigma_{\mathrm{ND}}(\Omega)$ at $\Omega = 0$, where the two beams have the same frequency $\omega_0 = \omega_{fi}/2$ and the non-degenerate configuration formally reduces to the degenerate one. Numerically, the expression (24) evaluated at $\Omega = 0$ gives

$$\sigma_{\mathrm{ND}}(0) \;=\; 1.16 \times 10^{-22}\ \mathrm{cm}^4/\mathrm{W}. \tag{31}$$

For comparison, the Doppler-free degenerate value reported by Caracas Núñez *et al.* [5] is

$$\sigma_D \;=\; 4.58 \times 10^{-21}\ \mathrm{cm}^4/\mathrm{W}, \tag{32}$$

so that the ratio between both values is

$$\frac{\sigma_{\mathrm{ND}}(0)}{\sigma_D} \;\approx\; 2.5 \times 10^{-2}. \tag{33}$$

The two numbers do not coincide, but the discrepancy is consistent with the approximations of the present model. In particular, the calculation of Ref. [5] includes the hyperfine structure of cesium (nuclear spin $I = 7/2$, with $F = 3, 4$ sublevels in both $6S_{1/2}$ and $8S_{1/2}$) and the associated coherent sum over magnetic sublevels through Wigner 6-j angular factors. None of these elements is incorporated in the present numerical implementation. The remaining difference can be reasonably attributed to the absence of the hyperfine and angular-momentum structure. Future work involves the inclusion of these factors to further refine the result.

D. Cross-Section Enhancement Near the $6P_{3/2}$ Resonance

The main motivation for studying the non-degenerate regime is the possibility of enhancing the TPA cross section by tuning one of the photon frequencies close to an intermediate transition. To quantify this effect, Figure 5 shows a zoom of $\sigma_{\mathrm{ND}}(\Omega)$ around the $6P_{3/2}$ resonance, located at $\Omega/2\pi \simeq 12.8$ THz.

Two specific configurations are highlighted on the plot. The first ($\Omega = 0$, $\lambda = 822$ nm) corresponds to the degenerate point of Section III C, with $\sigma_{\mathrm{ND}}(0) = 1.16 \times 10^{-22}\,\mathrm{cm}^4/\mathrm{W}$. The second corresponds to a non-degenerate configuration in which the two beams have wavelengths of 852 nm

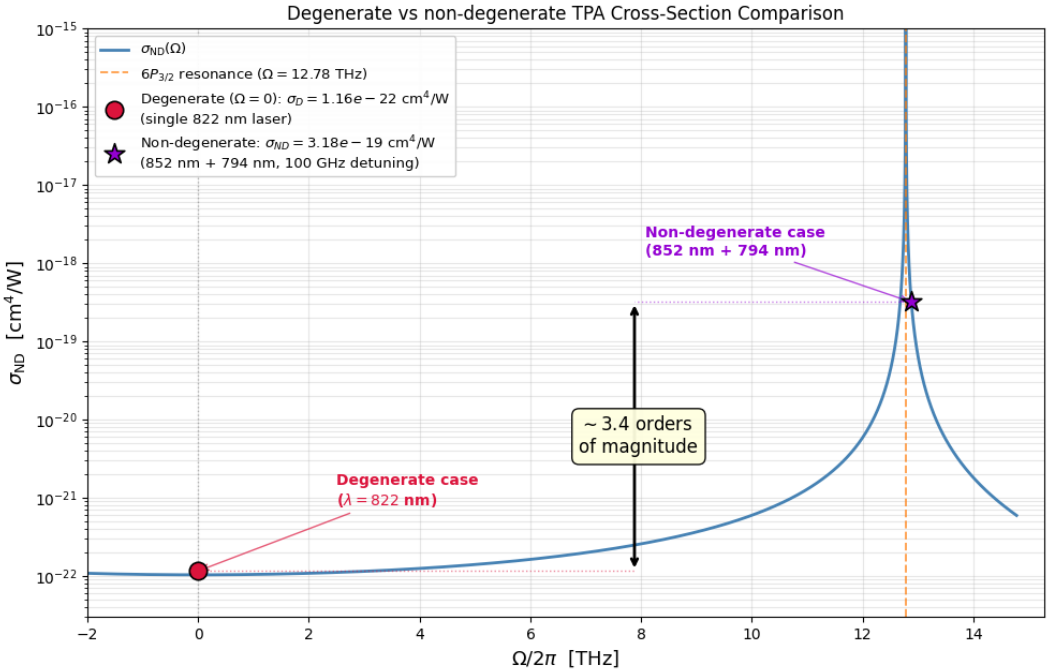

FIG. 5. Zoom of the non-degenerate cross section $\sigma_{\mathrm{ND}}(\Omega)$ around the $6P_{3/2}$ intermediate resonance. The red marker indicates the degenerate point ($\lambda = 822$ nm, $\Omega = 0$); the purple marker indicates the non-degenerate configuration at 852 nm + 794 nm ($\Omega/2\pi \simeq 12.8$ THz, equivalent to a 100 GHz detuning from the $6P_{3/2}$ transition), where the cross section is enhanced by approximately 3.4 orders of magnitude relative to the degenerate value.

and 794 nm, equivalent to a detuning of approximately 100 GHz with respect to the $6S_{1/2} \to 6P_{3/2}$ transition. At this point the numerical evaluation of Eq. (24) gives

$$\sigma_{\mathrm{ND}}^{(852+794)} \;\simeq\; 3.18 \times 10^{-19}\ \mathrm{cm}^4/\mathrm{W}, \tag{34}$$

which represents an enhancement of approximately

$$\frac{\sigma_{\mathrm{ND}}^{(852+794)}}{\sigma_{\mathrm{ND}}(0)} \;\approx\; 2.7 \times 10^{3} \;\simeq\; 3.4 \text{ orders of magnitude.} \tag{35}$$

This is the main result of the numerical analysis: keeping the same total photon energy as in the degenerate case, but redistributing it between two beams so that one of them sits near the $6P_{3/2}$ resonance, the predicted TPA cross section grows by more than three orders of magnitude. Such an enhancement, if reproduced experimentally, would translate directly into a similar increase in the two-photon-induced fluorescence signal, since the fluorescence count rate is proportional to σ for fixed beam intensities and atomic density.

IV. CONCLUSIONS AND FUTURE WORK

In this work an explicit expression for the non-degenerate TPA cross section $\sigma_{\mathrm{ND}}(\omega_1, \omega_2)$ for the $6S_{1/2} \to 8S_{1/2}$ transition in cesium atoms was derived from second-order time-dependent perturbation theory in the electric dipole approximation. The derivation made the role of the two indistinguishable time orderings of the absorption process explicit, leading to a transition probability with a quantum interference term $2\,\mathrm{Re}\, A_{12} A_{21}^{*}$. The resulting cross section [Eq. (24)] is naturally decomposed into four contributions: the global two-photon resonance, the two intermediate-state resonances, and a quantum-path interference term between different intermediate states.

The numerical evaluation of this expression for cesium, using the same atomic parameters as the degenerate calculation of Ref. [5], reproduces the predicted spectral structure: sharp Lorentzian peaks at the expected positions $\Omega_m = \pm(\omega_{mi} - \omega_0)$ for the four dominant intermediate states, $1/\delta^2$ tails far from the peaks, and Fano-like valleys between consecutive resonances. At $\Omega = 0$ the model reproduces the qualitative behaviour of the degenerate case; the quantitative difference with respect to the value reported in [5] is consistent with the fact that the hyperfine structure and the angular-momentum coupling have not been included in the present implementation. The main physical result is the prediction that a non-degenerate configuration in which one of the photons is tuned within ~ 100 GHz of the $6S_{1/2} \to 6P_{3/2}$ transition (specifically 852 nm + 794 nm) enhances σ_{ND} by approximately 3.4 orders of magnitude with respect to the degenerate point.

The continuation of this work has two complementary directions. On the theoretical side, the model must be extended to include the full hyperfine structure of cesium and the associated Wigner 6-j angular factors, following the same lines as the degenerate treatment of Refs. [5, 6]. On the experimental side, the predicted enhancement can be tested in the existing cesium vapor cell setup of the Quantum Optics laboratory by using two frequency-controlled diode lasers at 852 nm and 794 nm, and scanning their detuning around the $6P_{3/2}$ resonance while maintaining the two-photon resonance with the $8S_{1/2}$ level. Measuring the fluorescence signal as a function of the non-degeneracy parameter Ω would provide a direct experimental test of the central prediction of this work, and would also constitute a first step towards future non-degenerate ETPA experiments, in which the expected fluorescence rates are much smaller due to the low flux of entangled photon

pairs [12].

---

[1] M. Göppert-Mayer, *Über Elementarakte mit zwei Quantensprüngen*, Ann. Phys. **401**, 273–294 (1931).

[2] W. Kaiser and C. G. B. Garrett, *Two-Photon Excitation in CaF_2:Eu^{2+}*, Phys. Rev. Lett. **7**, 229–231 (1961).

[3] R. W. Boyd, *Nonlinear Optics*, 4th ed. (Academic Press, 2020).

[4] G. Grynberg and B. Cagnac, *Doppler-free multiphotonic spectroscopy*, Rep. Prog. Phys. **40**, 791–841 (1977).

[5] M. S. Caracas Núñez, M. A. Gonzalez, and M. Núñez Portela, *Theoretical and experimental study of the 6S-8S two-photon absorption cross-section in cesium atoms*, Opt. Express **31**, 31749–31759 (2023).

[6] M. S. Caracas Núñez, *Estudio Teórico y Experimental de la Sección Eficaz de Absorción de dos Fotones en Átomos de Cesio*, Monografía de grado, Departamento de Física, Universidad de los Andes, Bogotá, Colombia (2023).

[7] C.-Y. Cheng, C.-M. Wu, G. B. Liao, and W.-Y. Cheng, *Cesium $6S_{1/2} \rightarrow 8S_{1/2}$ two-photon-transition-stabilized 822.5 nm diode laser*, Opt. Lett. **32**, 563–565 (2007).

[8] J. E. Bjorkholm and P. F. Liao, *Resonant Enhancement of Two-Photon Absorption in Sodium Vapor*, Phys. Rev. Lett. **33**, 128–131 (1974).

[9] J. E. Bjorkholm and P. F. Liao, *Line shape and strength of two-photon absorption in an atomic vapor with a resonant or nearly resonant intermediate state*, Phys. Rev. A **14**, 751–760 (1976).

[10] T. M. True, G. A. Pitz, C. A. Rice, and G. P. Perram, *Resonant enhancement of two-photon absorption in rubidium with crossed polarizations*, Opt. Commun. **510**, 127943 (2022).

[11] U. Fano, *Effects of configuration interaction on intensities and phase shifts*, Phys. Rev. **124**, 1866–1878 (1961).

[12] M. G. Raymer, T. Landes, and A. H. Marcus, *Entangled two-photon absorption by atoms and molecules: A quantum optics tutorial*, J. Chem. Phys. **155**, 081501 (2021).